

Original Article

# *Azadirachta indica* -Mediated Synthesis of Iron Oxide Nanozymes with Superior Peroxidase-Like Catalytic Efficiency

Zahid H Shar<sup>1\*</sup>, Muqadus Abbasi<sup>1</sup>, Nusrat N Memon<sup>1</sup>, Anoosha Maryam<sup>1</sup>, Pawan Kumar<sup>1</sup>, Pirah Ismail<sup>1</sup>, Pirah Zahir<sup>1</sup>

<sup>1</sup> Dr.M.A Kazi institute of Chemistry, University of Sindh Jamshoro, Pakistan

\*Corresponding author: Zahid H Shar, [zahidshar\\_2009@yahoo.com](mailto:zahidshar_2009@yahoo.com)

## ABSTRACT

**Background:** Metal-based nanomaterials with natural enzyme-like activity, nanozymes are gaining popularity as alternatives to biological enzymes due to their superior stability and cost-effectiveness. The catalytic efficacy of iron oxide nanozymes may be diminished by aggregation during chemical production. **Objective:** This study aimed to synthesize iron oxide nanozymes using *Azadirachta indica* leaf extract and compare their structural composition and OPD–H<sub>2</sub>O<sub>2</sub> peroxidase-like catalytic activity with chemically synthesized nanozymes. **Methods:** Iron oxide nanozymes were synthesized using chemical co-precipitation and *Azadirachta indica*-mediated green synthesis. The synthesized materials were characterized by scanning electron microscopy (SEM) and energy-dispersive X-ray spectroscopy (EDS). Peroxidase-like activity was evaluated using oxidation of o-phenylenediamine (OPD) in the presence of hydrogen peroxide(H<sub>2</sub>O<sub>2</sub>). Kinetic parameters were estimated using Michaelis–Menten analysis. **Results:** Green-synthesized nanozymes showed comparatively reduced aggregation and lower residual chlorine signal than chemically synthesized nanozymes. *Azadirachta indica*-mediated nanozymes generated the maximum absorbance at 451 nm in the OPD–H<sub>2</sub>O<sub>2</sub> assay, suggesting more peroxidase-like activity. Kinetic analysis revealed that green-synthesized nanozymes had a higher V<sub>max</sub> and a roughly 5.4-fold higher V<sub>max</sub>/K<sub>m</sub>-based catalytic effectiveness than chemically synthesized nanozymes. **Conclusion:** Iron oxide nanozymes with enhanced catalytic performance were generated by *Azadirachta indica*-mediated synthesis, most likely as a result of phytochemical-assisted stabilization and surface modification. Before biosensing or environmental usage, additional phase characterization, replicate-based validation, and application-specific testing are needed.

**Keywords:** Green synthesis; *Azadirachta indica*; iron oxide nanozymes; peroxidase-like activity; OPD oxidation; catalytic efficiency.

**“Cite this Article”** | Received: 01 September 2025; Accepted: 13 December 2025; Published: 31 December 2025.

**Author Contributions:** ZHS: concept, design, supervision, and drafting; MA, NNM, AM, PK, and PI: data collection, analysis, and manuscript revision.

**Ethical Approval:** University of Sindh, Jamshoro, Pakistan. **Informed Consent:** Written informed consent was obtained from all participants; **Conflict**

**of Interest:** The authors declare no conflict of interest; **Funding:** No external funding; **Data Availability:** Available from the corresponding author on

reasonable request; **Acknowledgments:** The author sincerely thanks Professor Dr. Irfana Mallah, Director of the Dr. M.A. Kazi Institute of Chemistry,

University of Sindh, Jamshoro, for providing the necessary support and access to its laboratory facilities

## INTRODUCTION

Peroxidase enzymes frequently utilized in biosensing, colorimetric detection, biomedical tests, and environmental monitoring because they catalyse the oxidation of chromogenic substrates in the presence of hydrogen peroxide (1, 2). However, high production and purification costs, low operational stability, denaturation and decreased activity under storage conditions are common limitations in the utilization of natural enzymes (3, 4). Given these limitations, considerable attention has been directed

toward the development of nanozymes(5). These nanomaterials, which possess enzyme-like catalytic activity, offer enhanced stability, tunability, and cost-effectiveness over biological enzymes (6-8).

Iron oxide-based nanoparticles have gained significant attention among various nanozyme systems due to their inherent peroxidase-like activity, biocompatibility and magnetic behaviour which facilitate facile recovery from reaction systems (9-11). Chromogenic substrates like o-phenylenediamine (OPD), which is oxidized in the presence of hydrogen peroxide to form a yellow-coloured product (2,3-diaminophenazine) that can be measured spectrophotometrically, are frequently used to assess their catalytic activity (12, 13). Iron oxide nanozymes improve substrate oxidation in this reaction system by facilitating electron transport and encouraging the production of reactive oxygen species (14, 15). Despite their benefits, chemically produced iron oxide nanoparticles exhibit surface instability, aggregation, and uneven shape, which can lower catalytic performance by reducing the number of active sites (16, 17) Plant-derived phytochemicals, which can function as reducing, stabilizing and capping agents during nanoparticle synthesis, offer a sustainable alternative that eliminates the hazardous reagents employed in conventional methods (18, 19). This approach may enhance dispersion, reduce aggregation, and minimize residual chemical contaminants (20).

Neem, or *Azadirachta indica*, is a widely accessible medicinal plant that contains a variety of bioactive phytochemicals, such as terpenoids, flavonoids, polyphenols (21, 22). These components might aid in the regulated production and stabilization of iron oxide nanoparticles (23, 24). Few studies have been reported *Azadirachta indica*-mediated iron oxide nanozymes with chemically synthesized counterparts in terms of peroxidase-like activity and Michaelis-Menten kinetic behaviour, despite many reports of plant-mediated synthesis of metal oxide nanoparticles (25, 26). Therefore, this study aimed to synthesize iron oxide nanozymes using *Azadirachta indica* leaf extract and compare their structural composition and OPD-H<sub>2</sub>O<sub>2</sub> peroxidase-like catalytic activity with chemically synthesized nanozymes

## MATERIALS AND METHODS

All chemicals used in this study were of analytical grade. Ferric chloride hexahydrate, ferrous sulfate, ammonium hydroxide, sodium hydroxide, citric acid, ethanol, hydrogen peroxide, and o-phenylenediamine (OPD) were obtained from Sigma-Aldrich. Deionized water was used throughout all synthesis, washing, and assay procedures.

Chemically Iron oxide based nanozymes were synthesized by following the co-precipitation technique as described previously (27). Briefly, ferrous sulphate (0.01 M) and ferric chloride (0.02 M) aqueous solutions were combined in a reaction flask with continuous stirring, meanwhile, pH was adjusted to 11 with ammonium hydroxide, which results in the formation of iron oxide nanoparticles. The nano particles formed were separated by centrifuging the mixture at 4000 rpm, and cleaned with ethanol and deionized water. Purified nanozymes were dried for 24 hours at 60C in a hot air oven to produce a fine powder (28, 29).

for green synthesis, *Azadirachta indica* leaves were rinsed with water and air-dried in the shade for a week. The dried leaves were ground into a fine powder and its extract was formed by mixing 10 g of the powdered leaves was combined with 100 mL of water and heated to a temperature of 50-60 °C for 20 minutes, and filtered by using Whatman No. 40 (30). 50 mL of ferric chloride hexahydrate (0.1 M) and 50 mL of freshly prepared leaf extract was combined while continuously stirring and Sodium hydroxide solution (1 M) was added dropwise until the pH reached at 11, which results in formation of a black suspension (31). After spinning the mixture in a centrifuge for 15 minutes at a speed of 4000 rpm, the synthesized nanoparticles were thoroughly washed with water and ethanol to eliminate any unreacted materials and residual phytochemicals. The final product was then dried at 60 °C to obtain powdered *Azadirachta indica* mediated nanozymes.

The surface morphology and elemental composition of both chemically synthesized and *Azadirachta indica*-mediated iron oxide nanozymes were examined using scanning electron microscopy (SEM) and energy-dispersive X-ray spectroscopy (EDS). SEM was used to evaluate particle morphology, surface structure, and aggregation pattern, whereas EDS was used to determine the elemental composition of the synthesized nanomaterials, particularly the relative presence of iron, oxygen, and residual precursor-derived elements.

Peroxidase-like catalytic activity was assessed using the OPD–H<sub>2</sub>O<sub>2</sub> colorimetric reaction system. Three different pH 3.0, 4.0, and 5.0 were investigated using citrate buffer to check the effect of pH on the peroxidase activity (27, 32, 33). Peroxidase-like activity was measured colorimetrically in quartz cuvette containing citrate buffer (3.8 mL, pH 3-5), OPD solution (0.5 mL), and hydrogen peroxide (30% v/v) (0.3 mL). The oxidation of OPD to 2,3-diaminophenazine (DAP) was observed spectrophotometrically at 451 nm while the total reaction volume was kept at 4.8 mL (32). Furthermore, the effect of substrate concentration on catalytic efficiency was assessed at different OPD concentrations in the range of (10–25 mM) at constant optimized pH (3). Absorbance was measured at regular intervals over period of 30 minutes (34)

The effect of substrate concentration on catalytic activity was evaluated by performing reactions at different OPD concentrations ranging from 10 to 25 mM under the optimized pH condition. Absorbance at 451 nm was recorded at regular time intervals over 30 minutes. Initial reaction velocities were calculated from the linear portion of the absorbance-versus-time curves (35). Michaelis–Menten kinetic parameters were estimated by fitting the initial velocity data to the Michaelis–Menten equation:

$$V = \frac{V_{\max}[S]}{K_m + [S]}$$

where  $V$  represents the initial reaction velocity,  $V_{\max}$  is the maximum reaction velocity,  $[S]$  is the OPD substrate concentration, and  $K_m$  is the Michaelis constant. Lineweaver–Burk double-reciprocal plots were also used to support kinetic parameter estimation:

$$\frac{1}{V} = \frac{K_m}{V_{\max}} \frac{1}{[S]} + \frac{1}{V_{\max}}$$

Catalytic efficiency was calculated as  $V_{\max}/K_m$  for both nanozyme preparations. The calculated values were used to compare the catalytic performance of chemically synthesized and *Azadirachta indica*-mediated iron oxide nanozymes. Lower  $K_m$  was interpreted as higher apparent substrate affinity, whereas higher  $V_{\max}$  and  $V_{\max}/K_m$  indicated improved catalytic performance under the tested assay conditions.

## RESULTS

*Azadirachta indica*-mediated iron oxide nanozymes and chemically generated iron oxide nanozymes had distinct morphological structure as demonstrated by scanning electron microscopy presented in figure 1. Particle clustering during traditional co-precipitation synthesis was indicated by the chemically produced nanozymes' asymmetrical and aggregated shapes (Figure 1). The *Azadirachta indica*-mediated nanozymes, on the other hand, demonstrated significantly greater dispersion with less aggregation and more distinct particle morphologies. This is due to leaf extract's phytochemical components helped to stabilize the nanoparticles during production.

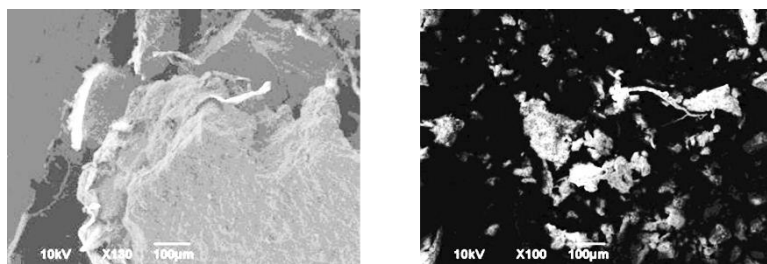


**Figure 1.** SEM morphology of iron oxide nanozymes synthesized by (A) chemical co-precipitation and (B) *Azadirachta indica*-mediated green synthesis.

Iron and oxygen were found in both synthetic nanozyme preparations as shown by energy-dispersive X-ray spectroscopy (Table 1). Chemically produced nanozymes displayed Fe and O peaks in addition to measurable chlorine, indicating residual precursor-derived chlorine as shown in figure 2. The nanozymes driven by *Azadirachta indica* exhibited a much lower chlorine content and a greater relative oxygen signal (Table 1). The elevated oxygen signal could be the result of oxygen-bearing functional groups connected to phytochemicals obtained from plants on the surface of the nanoparticles.

**Table 1.** Elemental composition of synthesized iron oxide nanozymes based on EDS analysis

Element	Chemically synthesized nanozymes, wt%	<i>Azadirachta indica</i> -mediated nanozymes, wt%
Oxygen (O)	60.13	94.81
Iron (Fe)	34.38	4.73
Chlorine (Cl)	5.49	0.46

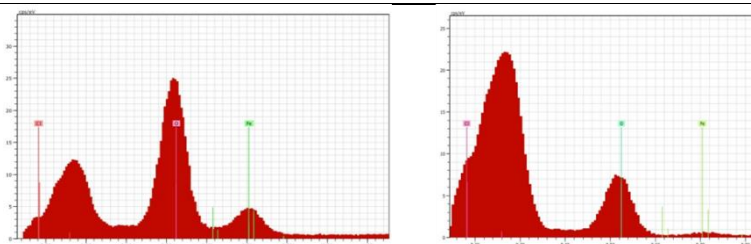


**Figure 2.** EDS spectra of iron oxide nanozymes synthesized by (A) chemical co-precipitation and (B) *Azadirachta indica*-mediated green synthesis.

Nanozymes' peroxidase-like catalytic activity was measured by extent of oxidation of OPD (OPD–H<sub>2</sub>O<sub>2</sub> system) to 2,3-diaminophenazine, a yellow-colored compound measured at 451 nm. The absorbance values obtained from the chemically synthesized, green synthesized, and uncatalyzed conditions are presented in Table 2. *Azadirachta indica*-mediated nanozymes produced the maximum absorbance peak at about 451 nm, whereas chemically created nanozymes increased absorbance in comparison to the uncatalyzed process suggests that the green-synthesized nanozyme exhibited more peroxidase-like activity under the studied conditions (figure 3)

**Table 2.** Comparative OPD oxidation response of synthesized nanozymes

Reaction system	Relative absorbance response at 451 nm	Interpretation
OPD + H <sub>2</sub> O <sub>2</sub> without nanozymes	Lowest	Minimal uncatalyzed oxidation
OPD + H <sub>2</sub> O <sub>2</sub> + chemically synthesized nanozymes	Intermediate	Catalytic OPD oxidation present
OPD + H <sub>2</sub> O <sub>2</sub> + <i>Azadirachta indica</i> -mediated nanozymes	Highest	Strongest peroxidase-like activity

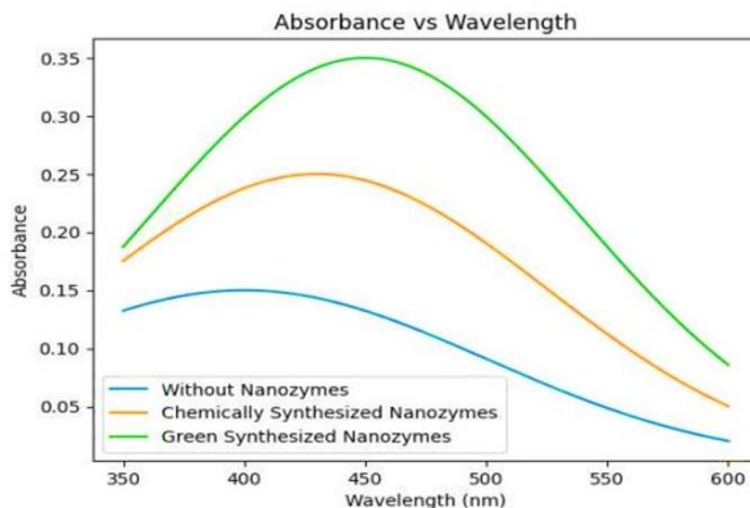


**Figure 3.** UV-visible absorbance spectra of OPD oxidation in the absence and presence of chemically synthesized and *Azadirachta indica*-mediated iron oxide nanozymes.

The kinetic parameters of the enzyme were evaluated using the Michaelis-Menten model, which serves as a fundamental framework for describing the rate of enzyme-catalyzed reactions as a function of substrate concentration(36). Linear area of absorbance-versus-time curves was used to determine initial reaction velocities and assess the impact of OPD concentration (10–25 mM) on peroxidase-like activity (Table 3). *Azadirachta indica*-mediated nanozymes consistently recorded 8–10 times greater velocities than chemically produced counterparts across all doses tested, as Figure 4A illustrates. Initial velocity rose gradually with OPD concentration for both nanozyme systems. Both systems exhibit classical hyperbolic Michaelis-Menten saturation dynamics, as shown in Figure 4B. *A. indica*-mediated nanozymes showed a greater  $V_{max}$  of  $7.0 \times 10^{-3} \text{ M s}^{-1}$  along with a  $K_m$  of 17.8 mM, while chemically manufactured nanozymes produced a  $K_m$  of 9.4 mM and  $V_{max}$  of  $6.8 \times 10^{-4} \text{ M s}^{-1}$ . The Lineweaver-Burk double-reciprocal plot is shown in Figure 4C, where both systems generated linear fits verifying enzyme-mimetic behavior in line with a ping-pong catalytic mechanism. Superior catalytic throughput is visibly confirmed by the green nanozyme line's flatter slope and lower y-intercept. The catalytic efficiency ( $V_{max}/K_m$ ) for chemical and green-synthesized nanozymes was  $7.23 \times 10^{-1}$  and  $3.93 \times 10^{-1}$ , respectively, as shown in Table 3. This is a 5.4-fold improvement due to the enhanced surface morphology and decreased aggregation provided by *Azadirachta indica* phytochemicals.

**Table 3.** Kinetic parameters of chemically synthesized and *Azadirachta indica*-mediated iron oxide nanozymes

Catalyst	Substrate	$K_m$ (mM)	$V_{max}$ (M $s^{-1}$ )	$V_{max}/K_m$	Relative Catalytic Efficiency
Chemically synthesized iron oxide nanozymes	OPD	9.4	$6.8 \times 10^{-4}$	$7.23 \times 10^{-5}$	1.0
<i>Azadirachta indica</i> -mediated iron oxide nanozymes	OPD	17.8	$7.0 \times 10^{-3}$	$3.93 \times 10^{-4}$	5.4

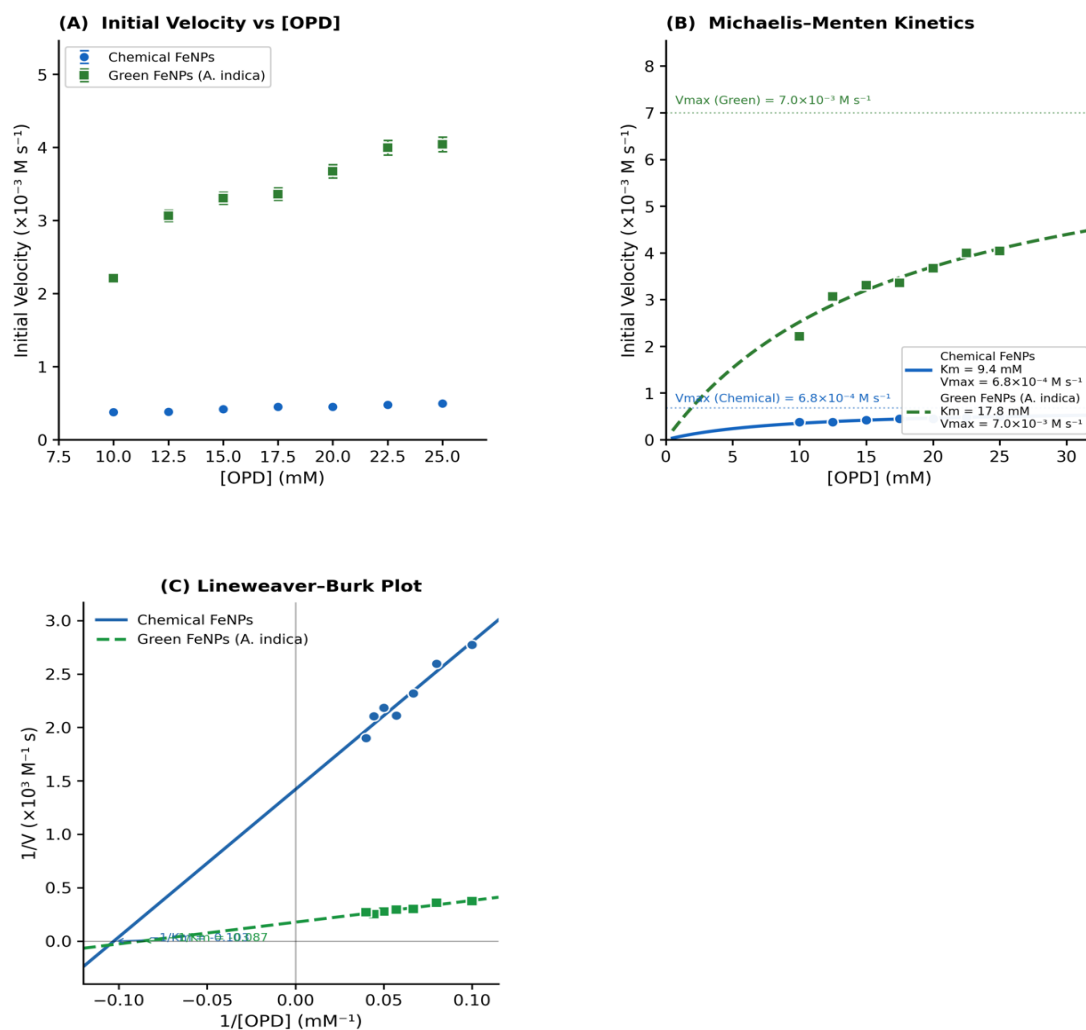


Figure 4: Kinetic analysis of peroxidase like activity: chemical vs green-synthesized iron oxide nanozymes

## DISCUSSION

*Azadirachta indica*-mediated green synthesis produced iron oxide nanozymes with enhanced peroxidase-like catalytic performance. Green-synthesized nanozymes had a roughly 5.4-fold greater predicted catalytic efficiency based on  $V_{max}/K_m$ , stronger OPD oxidation at 451 nm, lesser residual chlorine signal on EDS, and comparatively less aggregation on SEM. This can be explained by known function of phytochemicals derived from plants as stabilizing and surface-modifying agents during the creation of nanoparticles as explained in many studies (37-39). The *Azadirachta indica*-mediated technique provided greater dispersion, while chemical co-precipitation method created more irregular and aggregated structures as shown in SEM images. This distinction is important because surface accessibility, particle aggregation, and the availability of catalytic sites all have a significant impact on nanozyme activity(40). Reduced aggregation in green-synthesized nanozymes enhances catalytic performance by increasing the effective surface area available for interaction with OPD and  $\text{H}_2\text{O}_2$  (41, 42).

EDS analysis confirmed the presence of iron and oxygen in both nanozyme formulations, while the green-synthesized sample exhibited significantly lower chlorine content than the chemically synthesized one, likely due to residual chloride from the ferric chloride precursor. Oxygen-containing functional groups from phytochemicals adsorbed on the nanoparticle surface may be the cause of the increased relative oxygen signal in the green-synthesized sample, in line with the findings of (37), who linked surface-adsorbed organic biomolecules to increased oxygen signals in plant-capped iron oxide nanoparticles. This lends credence to the idea that proteins derived from plants could cap the surface

(43). Both nanozyme preparations improved OPD oxidation as compared to the uncatalyzed process, according to the OPD–H<sub>2</sub>O<sub>2</sub> colorimetric assay, with the *Azadirachta indica*-mediated nanozymes exhibiting the highest absorbance. This outcome aligns with the fundamental research of (27), who initially revealed that Fe<sub>3</sub>O<sub>4</sub> nanoparticles have intrinsic peroxidase-like activity and catalyze the oxidation of chromogenic substrates mediated by H<sub>2</sub>O<sub>2</sub> through electron-transfer and reactive oxygen species production. Improved particle dispersion, changed surface chemistry, and easier access to catalytic sites could all contribute to the green-synthesized nanozymes' higher absorbance response. The peroxidase mechanism that underlies this activity has been further clarified by (14), who showed that Fe<sup>2+</sup> within Fe<sub>3</sub>O<sub>4</sub> transfers electrons to the surface via the Fe<sup>2+</sup>–O–Fe<sup>3+</sup> chain, regenerating surface Fe<sup>2+</sup> and sustaining the catalytic reaction(44). This mechanism functions best in acidic environments, which is consistent with the pH 3.0 optimum found in the current study.

The green-synthesized nanozymes' increased catalytic capacity is further supported by the kinetic study. Initial reaction velocities were obtained from the linear region of absorbance-versus-time curves at various OPD concentrations (Figure 4A) and fitted to the hyperbolic Michaelis-Menten equation (Figure 4B), in accordance with the standardized Michaelis-Menten kinetic framework for peroxidase-like nanozymes described by(45). Both systems exhibit conventional enzyme-mimetic kinetics compatible with a ping-pong catalytic mechanism, as previously demonstrated for Fe<sub>3</sub>O<sub>4</sub> nanozymes by the Lineweaver–Burk double-reciprocal linearization (Figure 4C) (45). Under the measured OPD concentrations, the *Azadirachta indica*-mediated nanozymes had a larger V<sub>max</sub> than chemically generated nanozymes, indicating stronger maximal catalytic activity. The green-synthesized nanozymes, however, also had a larger K<sub>m</sub> (17.8 mM versus 9.4 mM), indicating a decreased apparent substrate affinity for OPD. Consequently, the data show that, despite decreased apparent affinity, green synthesis mainly increased maximum catalytic capacity and overall V<sub>max</sub>/K<sub>m</sub>-based catalytic efficiency. This pattern is consistent with surface-functionalized nanozymes, where increased active site density coexists with partial steric shielding by surface-bound organic molecule (42). Catalytic efficiency (V<sub>max</sub>/K<sub>m</sub>) was roughly 7.23 × 10<sup>-1</sup> for chemically synthesized nanozymes and 3.93 × 10<sup>-2</sup> for *Azadirachta indica*-mediated nanozymes, as shown in Table 3. This represents a roughly 5.4-fold increase due to the enhanced surface morphology and phytochemical capping provided by *A. indica* leaf extract (27, 37).

## CONCLUSION

Iron oxide nanozymes with better dispersion, less residual chlorine signal, and greater OPD–H<sub>2</sub>O<sub>2</sub> peroxidase-like activity were successfully created via *Azadirachta indica*-mediated green synthesis compared to their chemically synthesized counterparts. Although their higher K<sub>m</sub> indicated a lower apparent OPD affinity under the testing conditions, kinetic analysis revealed that the green-synthesized nanozymes had a higher V<sub>max</sub> and around 5.4-fold larger V<sub>max</sub>/K<sub>m</sub>-based catalytic efficiency. These results imply that *Azadirachta indica* leaf extract could be a useful stabilizing and surface-modifying agent for the synthesis of iron oxide nanozymes that are catalytically active. Before these nanozymes may be developed for biosensing or environmental applications, more structural characterization, replicate-based kinetic validation, and application-specific testing are necessary.

## References

1. Kyomuhimbo HD, Feleni U, Haneklaus NH, Brink H. Recent advances in applications of oxidases and peroxidases polymer-based enzyme biocatalysts in sensing and wastewater treatment: a review. *Polymers*. 2023;15(16):3492.
2. Hamid M. Potential applications of peroxidases. *Food chemistry*. 2009;115(4):1177–86.
3. Sanchez-Tirado E, Yanez-Sedeno P, Pingarron JM. Carbon-based enzyme mimetics for electrochemical biosensing. *Micromachines*. 2023;14(9):1746.
4. Kabir MF, Ju L-K. On optimization of enzymatic processes: Temperature effects on activity and long-term deactivation kinetics. *Process Biochemistry*. 2023;130:734–46.
5. Ai Y, Hu ZN, Liang X, Sun Hb, Xin H, Liang Q. Recent advances in nanozymes: from matters to bioapplications. *Advanced Functional Materials*. 2022;32(14):2110432.

6. Phan-Xuan T, Breitung B, Dailey LA. Nanozymes for biomedical applications: Multi-metallic systems may improve activity but at the cost of higher toxicity? *Wiley Interdisciplinary Reviews: Nanomedicine and Nanobiotechnology*. 2024;16(4):e1981.
7. Singh S. Nanomaterials exhibiting enzyme-like properties (nanozymes): current advances and future perspectives. *Frontiers in chemistry*. 2019;7:46.
8. Wu J, Wang X, Wang Q, Lou Z, Li S, Zhu Y, et al. Nanomaterials with enzyme-like characteristics (nanozymes): next-generation artificial enzymes (II). *Chemical Society Reviews*. 2019;48(4):1004–76.
9. Ghazzy A, Nsairat H, Said R, Sibai OA, AbuRuman A, Shraim AS. Magnetic iron oxide-based nanozymes: from synthesis to application. *Nanoscale Advances*. 2024;6(6):1611–42.
10. Tanawish, Jahan N, Rasheed K, Iqbal M, Atif M. Exploring the advanced synthesis strategies and biomedical applications of iron oxide-based nanozymes: a comprehensive review. *Journal of Cluster Science*. 2024;35(8):2637–61.
11. Liu Q, Zhang A, Wang R, Zhang Q, Cui D. A review on metal-and metal oxide-based nanozymes: properties, mechanisms, and applications. *Nano-micro letters*. 2021;13(1):154.
12. Kim S-W, Lee WK, Lee J-S. Revisiting o-Phenylenediamine as a Nanomaterial-Catalyzed Signaling Agent: Dimerization versus Polymerization. *ACS omega*. 2023;8(48):46267–75.
13. Mazhani M. Development of silver-magnetite nanocomposites for cysteine sensing and dye degradation: Botswana International University of Science and Technology (Botswana); 2020.
14. Dong H, Du W, Dong J, Che R, Kong F, Cheng W, et al. Depletible peroxidase-like activity of Fe<sub>3</sub>O<sub>4</sub> nanozymes accompanied with separate migration of electrons and iron ions. *Nature Communications*. 2022;13(1):5365.
15. Yi Z, Yang X, Liang Y, Chapelin F, Tong S. Enhancing ROS-inducing nanozyme through intraparticle electron transport. *Small*. 2024;20(6):2305974.
16. Hasan YR, Faizal Wong FW, Ashari SE, Halim M, Mohamad R. Iron oxide nanoparticles: biosynthesis, peroxidase-like activity, and biosafety. *Applied Microbiology and Biotechnology*. 2025;109(1):202.
17. Zhu N, Ji H, Yu P, Niu J, Farooq M, Akram MW, et al. Surface modification of magnetic iron oxide nanoparticles. *Nanomaterials*. 2018;8(10):810.
18. Villagrán Z, Anaya-Esparza LM, Velázquez-Carriles CA, Silva-Jara JM, Ruvalcaba-Gómez JM, Aurora-Vigo EF, et al. Plant-based extracts as reducing, capping, and stabilizing agents for the green synthesis of inorganic nanoparticles. *Resources*. 2024;13(6):70.
19. Mohan A, Rajendran S, Palani N. Sustainable synthesis of iron oxide nanoparticles using phytochemicals: mechanisms, functionalization strategies, applications and future perspectives. *Material Sci & Eng*. 2025;9(2):36–54.
20. Singh H, Desimone MF, Pandya S, Jasani S, George N, Adnan M, et al. Revisiting the green synthesis of nanoparticles: uncovering influences of plant extracts as reducing agents for enhanced synthesis efficiency and its biomedical applications. *International journal of nanomedicine*. 2023;4727–50.
21. Tufail T, Bader Ul Ain H, Ijaz A, Nasir MA, Ikram A, Noreen S, et al. Neem (*Azadirachta indica*): A Miracle Herb; Panacea for All Ailments. *Food science & nutrition*. 2025;13(9):e70820.
22. Adhikari AS. PHYTOCHEMICALS AND ANTIOXIDANT ACTIVITIES OF NEEM (*Azadirachta indica*) LEAVES: Department of Nutrition & Dietetics Central Campus of Technology Institute ...; 2022.
23. Zambri NDS, Taib NI, Abdul Latif F, Mohamed Z. Utilization of neem leaf extract on biosynthesis of iron oxide nanoparticles. *Molecules*. 2019;24(20):3803.
24. Amstad E, Textor M, Reimhult E. Stabilization and functionalization of iron oxide nanoparticles for biomedical applications. *Nanoscale*. 2011;3(7):2819–43.
25. Rathore A, Devra V. *Azadirachta indica* leaf mediated synthesis of iron nanoparticles and their catalytic application in methylene blue degradation. *Catalysis Research*. 2023;3(1):1–12.
26. Kumari P, Devi L, Kadian R, Waziri A, Alam MS. Eco-friendly synthesis of *Azadirachta indica*-based metallic nanoparticles for biomedical application & future prospective. *Pharmaceutical Nanotechnology*. 2025;13(3):448–64.
27. Gao L, Zhuang J, Nie L, Zhang J, Zhang Y, Gu N, et al. Intrinsic peroxidase-like activity of ferromagnetic nanoparticles. *Nature nanotechnology*. 2007;2(9):577–83.
28. Sun S, Zeng H. Size-controlled synthesis of magnetite nanoparticles. *Journal of the American Chemical Society*. 2002;124(28):8204–5.

29. Wu W, He Q, Jiang C. Magnetic iron oxide nanoparticles: synthesis and surface functionalization strategies. *Nanoscale research letters*. 2008;3(11):397.
30. Sharma VK, Yngard RA, Lin Y. Silver nanoparticles: green synthesis and their antimicrobial activities. *Advances in colloid and interface science*. 2009;145(1-2):83–96.
31. Kharissova OV, Kharisov BI, Oliva Gonzalez CM, Méndez YP, López I. Greener synthesis of chemical compounds and materials. *Royal Society open science*. 2019;6(11).
32. Wei H, Wang E. Nanomaterials with enzyme-like characteristics (nanozymes): next-generation artificial enzymes. *Chemical Society Reviews*. 2013;42(14):6060–93.
33. Jv Y, Li B, Cao R. Positively-charged gold nanoparticles as peroxidase mimic and their application in hydrogen peroxide and glucose detection. *Chemical communications*. 2010;46(42):8017–9.
34. Lin Y, Ren J, Qu X. Catalytically active nanomaterials: a promising candidate for artificial enzymes. *Accounts of chemical research*. 2014;47(4):1097–105.
35. Cornish-Bowden A. *Fundamentals of enzyme kinetics*: John Wiley & Sons; 2013.
36. Golekar SM. Kinetic Modeling of Enzyme-Catalyzed Reactions Insights and Applications. *International Journal of Advanced Research and Multidisciplinary Trends (IJARMT)*. 2024;1(2):305–17.
37. Mahdavi M, Ahmad MB, Haron MJ, Namvar F, Nadi B, Rahman MZA, et al. Synthesis, surface modification and characterisation of biocompatible magnetic iron oxide nanoparticles for biomedical applications. *Molecules*. 2013;18(7):7533–48.
38. Edayadulla N, Sundari CS. Role of stabilizing agent role in nanomaterials (NM). *Sustainable green synthesised nano-dimensional materials for energy and environmental applications*: CRC Press; 2024. p. 47–63.
39. Trendafilova I, Popova M. Porous silica nanomaterials as carriers of biologically active natural polyphenols: effect of structure and surface modification. *Pharmaceutics*. 2024;16(8):1004.
40. Huang Y, Ren J, Qu X. Nanozymes: classification, catalytic mechanisms, activity regulation, and applications. *Chemical reviews*. 2019;119(6):4357–412.
41. Besenhard MO, LaGrow AP, Hodzic A, Kriechbaum M, Panariello L, Bais G, et al. Coprecipitation synthesis of stable iron oxide nanoparticles with NaOH: New insights and continuous production via flow chemistry. *Chemical Engineering Journal*. 2020;399:125740.
42. Laurent S, Forge D, Port M, Roch A, Robic C, Vander Elst L, et al. Magnetic iron oxide nanoparticles: synthesis, stabilization, vectorization, physicochemical characterizations, and biological applications. *Chemical reviews*. 2008;108(6):2064–110.
43. Choi Y, Kang G, Kim S, Cho Y, Oh J, Kim D, et al. Multiscale materials imaging and spectroscopy for battery materials. *EcoMat*. 2025;7(5):e70016.
44. Zhang Y, Dong H, Du W, Dong J, Kong F, Cheng W, et al. Depletable Peroxidase-like Activity of Fe<sub>3</sub>O<sub>4</sub> Nanozymes Accompanied with Phase Transformation Triggered by Separate Migration of Electron and Iron Ion. 2022.
45. Jiang B, Duan D, Gao L, Zhou M, Fan K, Tang Y, et al. Standardized assays for determining the catalytic activity and kinetics of peroxidase-like nanozymes. *Nature protocols*. 2018;13(7):1506–20.